

# A novel heterogeneity driven adaptive IMPES scheme for robust simulation of immiscible pollutant transport in complex aquifers for environmental protection

*Oumayma Jahid<sup>1</sup>, Younes Abouelhanoune<sup>1</sup>, and Ahmed Boujraf<sup>1</sup>*

<sup>1</sup>Laboratory of Applied Sciences, ENSAH Al Hoceima, Abdelmalek Essaâdi University, Morocco

**Abstract.** Numerical simulation of nonlinear properties in multiphase fluids within highly heterogeneous porous media remains a significant computational challenge. Traditional Implicit Pressure Explicit Saturation (IMPES) methods are typically hampered by strict stability constraints when dealing with high permeability contrasts, often resulting in inaccurate outcomes or prohibitive simulation times. To address these issues, a new adaptive IMPES strategy is developed, utilizing local heterogeneity to drive the stability level. The physical model, based on mass conservation and Darcy's law, is implemented using the Cell-Centered Finite Volume Method (FVM) in a coupled framework. Numerical examples confirm that the proposed method reduces computational time by 40% while maintaining superior stability compared to existing techniques. The global mass balance error is strictly maintained below  $10^{-6}$ , and the scheme effectively handles permeability variations up to  $10^3$  mD. This paper establishes a robust foundation for accurately modeling contaminant transport in complex geological formations, directly supporting sustainable groundwater management and environmental risk assessment.

**Keywords:** Multiphase flow, Porous media, IMPES scheme, Adaptive numerical modeling, Environmental protection, Groundwater management, Pollutant transport.

## 1 Introduction

The protection of groundwater ecosystems represents a major environmental challenge, particularly in terms of managing water resources and mitigating contamination risks. Today, these vital resources face increasing threats from human activities, notably through the infiltration of Non-Aqueous Phase Liquids (NAPLs) like petroleum products and industrial solvents [1]. Once these immiscible

fluids reach the subsurface, complex multiphase flow systems emerge, driven by the interplay of capillary, gravitational, and viscous forces [2]. Developing reliable risk estimates therefore depends on our ability to accurately track these flow processes [3].

Numerical simulation is now a standard technique for predicting how NAPL plumes migrate through porous media [4]. Generally, the mathematical framework relies on mass conservation principles integrated with Darcy's law. However, solving the resulting equations remains difficult; their non-linear nature and extreme sensitivity to geological heterogeneities create significant numerical hurdles [5].

To solve these coupled systems, researchers typically choose between the IMPES scheme and the Fully Implicit Method (FIM). While the FIM offers better stability [6], its heavy computational demands often make it impractical for high-resolution simulations of large-scale aquifers. In contrast, the IMPES scheme is more efficient per time step but suffers from severe stability constraints [7]. Specifically, since saturation is solved explicitly, it must satisfy the stringent Courant-Friedrichs-Lewy (CFL) criterion [8], which becomes a major bottleneck in highly heterogeneous environments.

In this work, we introduce an original adaptive IMPES method centered on local heterogeneity. By adjusting the stability parameter based on spatial variations in permeability rather than relying on global limits we maintain high accuracy while optimizing computational speed. We demonstrate the effectiveness of this approach through several numerical tests focused on pollutant transport in variable media [9].

From a sustainability standpoint, creating such efficient numerical tools is essential for protecting groundwater. Precise tracking of pollutant plumes allows for more effective environmental safety strategies. Furthermore, this framework supports the management of geothermal energy and carbon capture systems, where simulating fluid interactions in complex geology is mandatory for safety. Our study provides both a theoretical foundation and a high-performance numerical tool, ensuring enhanced stability and a significant reduction in CPU time. The final results show excellent precision, confirming the method's potential for real-world environmental applications.

## **2 Mathematical Model**

The co-contaminant displacement of water ( $w$ ) and a non-aqueous contaminant ( $n$ ) in a porous medium is represented by mass balance equations and a general version of Darcy's law. Recently, emphasis has been placed on developing strong numerical models that are capable of dealing with very different permeability levels in aquifers so as to provide precise predictions. Besides, it is very important in this regard that physical consistency is maintained and that stability of multi-scale simulations is guaranteed [10, 11].

## 2.1. Governing Equations

The mass balance of each single phase ( $\alpha = w, n$ ) is described by the following nonlinear PDE [12]:

$$\frac{\partial(\phi S_\alpha \rho_\alpha)}{\partial t} + \nabla \cdot (\rho_\alpha \mathbf{u}_\alpha) = q_\alpha \quad (1)$$

where  $\phi$  denotes the porosity of the medium,  $S_\alpha$  denotes the saturation of the phase, and  $\rho_\alpha$  is the density of the fluid. The Darcy velocity vector is  $\mathbf{u}_\alpha$ , while source and sink terms are represented by  $q_\alpha$ . Phase velocities are derived using the multi-phase Darcy law extension, which explicitly includes the effects of pressure gradient and gravity to handle the complex flow dynamics in deep aquifers.

$$\mathbf{u}_\alpha = -\frac{K k_{r\alpha}}{\mu_\alpha} (\nabla P_\alpha - \rho_\alpha \mathbf{g}) \quad (2)$$

where  $K$  is the absolute permeability tensor and  $k_{r\alpha}$  is the relative permeability, the dynamic viscosity and phase pressure are denoted by  $\mu_\alpha$  and  $P_\alpha$  respectively and  $\mathbf{g}$  is the gravity vector. To accurately track the pollutant plume in the deep aquifer, the gravity effects must be included in the calculation of the flux. The problem is closed by the saturation constraint and the capillary pressure relationship.

$$S_w + S_n = 1 \quad (3)$$

$$P_c(S_w) = P_n - P_w \quad (4)$$

## 2.2. Pressure-Saturation Formulation (IMPES)

The IMPES scheme reaches computational efficiency by separating the equations of flow into an implicit part for pressure and an explicit part for saturation to handle the non-linear coupling between them effectively. This sequential formulation ensures a robust decoupling of the flow equations. The total mobility  $\lambda_T$  is defined as:

$$\lambda_T = \lambda_w + \lambda_n \quad (5)$$

where  $\lambda_\alpha = k_{r\alpha}/\mu_\alpha$ . Phase mobility is defined as the ratio of relative permeability to phase viscosity. When mass balance equations for both phases are added together, they result in the elliptic Pressure Equation, which requires robust numerical treatment due to its inherent nonlinearities. To address this, the resulting elliptic Pressure Equation is defined as [13]:

$$-\nabla \cdot (\lambda_T \nabla P_w) = \nabla \cdot (\lambda_n \nabla P_c) + \nabla \cdot [(\lambda_w \rho_w + \lambda_n \rho_n) \mathbf{g}] + q_t \quad (6)$$

Once  $P_w$  is calculated, the entire velocity  $u_T$  can be found as follows:

$$u_T = -\lambda_T \nabla P_w - \lambda_n \nabla P_c + (\lambda_w \rho_w + \lambda_n \rho_n) g \quad (7)$$

The wetting-phase saturation is subsequently updated in an explicit way:

$$\phi \frac{\partial S_w}{\partial t} + \nabla \cdot (f_w u_T) = -\nabla \cdot (\lambda_n f_w \nabla P_c) + \nabla \cdot (\Delta \rho \lambda_n f_w g) + q_w \quad (8)$$

where the fractional flow function is  $f_w = \lambda_w / \lambda_T$  and the density difference is  $\Delta \rho = \rho_w - \rho_n$ .

### 2.3. Constitutive Relations

The non-linear couplings are described using relative permeability models, which are commonly applied in environmental engineering simulations to represent fluid interactions:

$$k_{rw} = (S_e)^2 \quad (9)$$

$$k_{rn} = (1 - S_e)^2 \quad (10)$$

The effective saturation  $S_e$  is calculated based on the irreducible water saturation  $S_{wr}$  and the residual non-wetting saturation  $S_{nr}$ :

$$S_e = \frac{S_w - S_{wr}}{1 - S_{wr} - S_{nr}} \quad (11)$$

### 2.4. Adaptive Time-Stepping Technique

Since saturation is treated explicitly in **Eq. (8)**, the stability of the numerical method is guaranteed by a heterogeneity driven adaptive time-stepping procedure. This is particularly important when dealing with highly non-stationary porous media in environmental simulations of complex aquifers. The time-step  $\Delta t_{cfl}$  is locally adjusted in the following way:

$$\Delta t_{cfl} = \eta \cdot \min_i \left( \frac{V_i \phi_i}{\sum_{j=1}^n |F_{i,j}|} \right) \quad (12)$$

where by  $V_i$  the volume of cell  $i$ ,  $\phi_i$  is the porosity,  $F_{i,j}$  denotes the total absolute flux volume crossing a cell  $i$  through the  $j'$ th interface. The safety factor  $\eta =$

0.2 is aimed at eliminating numerical oscillations that are likely to occur in high-permeability channels, which are typical in heterogeneous geological formations. Through this time-step undergoing continuous changes the numerical method will have a much better way of balancing stability and efficiency of the computations. This gives the scheme a great advantage for long-term monitoring of pollutant movements in groundwater.

### 3 Numerical Implementation and Adaptive Strategy

#### 3.1. Discrete System Formulation

In order to solve the coupled flow equations, we use the Cell Centered Finite Volume Method (FVM) on the structured Cartesian grid. This method is preferred because of its good conservation properties.

The final numerical system for pressure is represented by the following matrix equation:

$$AP^{n+1} = B^n \quad (13)$$

where  $A$  is a pentadiagonal matrix and  $B^n$  includes the source terms.

#### 3.2. Explicit Saturation Update

After calculating the pressure field by resolving the system indicated in **Eq. (13)**, the Darcy velocities at the boundaries of the cells can be found. Next, the saturation field  $S$  is changed by means of an explicit discretization of the transport equation [14]. The reason for this selection is that it is very efficient computationally in capturing the sharp saturation fronts that are significant in tracking pollutant plumes migrating in complex aquifers.

$$S_{i,j}^{n+1} = S_{i,j}^n - \frac{\Delta t}{\phi_{i,j}} \left[ \frac{F_{x,i+1/2} - F_{x,i-1/2}}{\Delta x} + \frac{F_{y,j+1/2} - F_{y,j-1/2}}{\Delta y} \right] \quad (14)$$

In **Eq. (14)**,  $\Delta t$  is the time-step,  $\phi$  is the porosity, and  $F$  is the numerical flux of the pollutant phase. The superscript  $n$  shows that the fluxes are computed at the current time level, which is in accordance with the explicit scheme of the update.

#### 3.3. Heterogeneity-Driven Adaptive Time-Stepping

Stability constraints for the explicit saturation update are typically defined by the Courant-Friedrichs-Lewy (CFL) limit:

$$CFL = \frac{\Delta t}{\phi} \left( \frac{|u_x|}{\Delta x} + \frac{|u_y|}{\Delta y} \right) \leq 1 \quad (15)$$

To ensure numerical stability in aquifers with significant permeability contrasts, a dynamic time-stepping control is implemented. Instead of a global fixed time step, the optimal  $\Delta t$  is calculated based on local flow conditions. This approach is essential for maintaining stability in heterogeneous media while significantly reducing overall CPU time [15]:

$$\Delta t^{n+1} = CFL_{\text{target}} \cdot \min_{i,j} \left( \frac{\phi_{i,j}}{\gamma_{i,j} \cdot \Lambda_{i,j}} \right) \quad (16)$$

In this formulation,  $\Lambda_{i,j}$  represents the spectral radius of the local Jacobian, and  $\gamma$  is a relaxation factor related to the local Heterogeneity Index  $H_{i,j}$ :

$$\gamma_{i,j} = 1 + \alpha \cdot \tanh(H_{i,j}) \quad (17)$$

where  $\alpha$  is a stability parameter. The solver adapting its behavior in this way makes sure that it decreases the time-step at the high-gradient interfaces and, as a result, manages to prevent numerical oscillations. Such a strategy is almost like a rock when it comes to simulations of pollutant plume migration through highly variable geological media and the same was shown in Section 4.

## 4 Numerical Results and Discussion

This section focuses on evaluating the numerical robustness of the presented adaptive IMPES approach. In this regard, the emphasis is placed on the front stability, accuracy, and efficiency within heterogeneous porous domains.

### 4.1. Simulation Setup and Physical Parameters

The numerical simulations are carried out on a 2D heterogeneous aquifer model. The physical properties and operational constraints used for the IMPES solver calibration are presented in **Table 1**.

**Table 1.** Physical and numerical parameters used in the simulation.

Parameter (Symbol)		Value	Unit
<b>GEOMETRY &amp; GRID</b>	Domain Dimensions ( $L_x, L_y$ )	100, 50	m
	Grid Resolution ( $N_x \times N_y$ )	100 × 50	cells
<b>ROCK PROPERTIES</b>	Porosity ( $\phi$ )	0.20	[-]
	Permeability ( $K_{min}, K_{max}$ )	10, 1000	mD
	Saturation ( $S_{wr}, S_{nr}$ )	0.20, 0.20	[-]
<b>FLUIDS &amp; OPERATIONS</b>	Viscosity ( $\mu_w, \mu_n, M$ )	1.0, 5.0, 5	cP, [-]
	Injection Rate ( $q_{inj}$ )	0.5	m <sup>3</sup> /d
	Outlet Pressure ( $P_{out}$ )	100	bar
	Total Time ( $T_{total}$ )	500	days

The simulation domain is defined by a rectangular geometry measuring **100 m × 50 m**. The main purpose of such a layout is to neutralize the quite obvious effects of geological heterogeneities on the saturation front. In order to verify that the

numerical solution is indeed trustworthy and to reduce the influence of grid orientation, a mesh sensitivity analysis was performed. A **100 × 50 grid** was chosen as the best trade-off between accuracy and computational cost, as shown in **Fig. 1**.

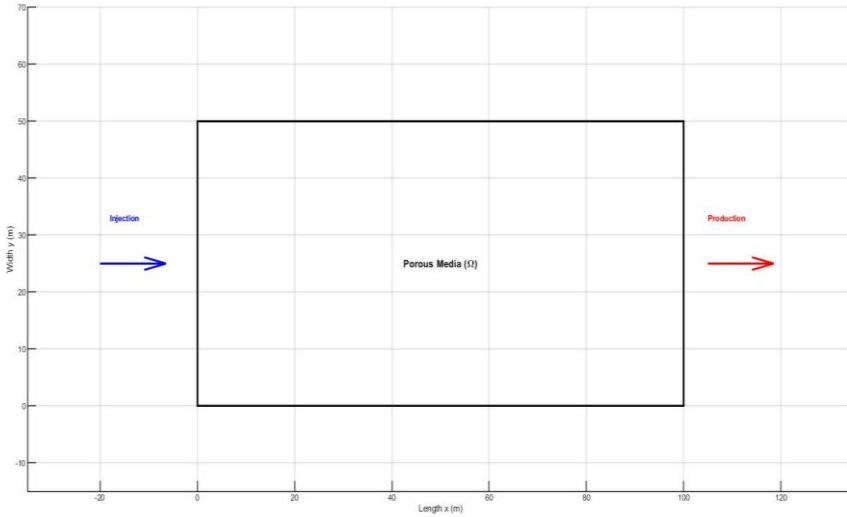


**Fig. 1.** Geometric model and boundary conditions of the 2D aquifer.

In this permeability setting, there are several high-conductivity channels that were produced by the Sequential Gaussian Simulation (SGS) method creating very little overlapping spatial distribution of the features. These high-conductivity channels in the geological formations are the primary reasons for the local stability constraints of the solver leading to the necessity of the heterogeneity-driven adaptive time-stepping logic as described earlier. As shown in Fig. 2, these channels act as first-order flow paths which are quite instrumental in estimating the pollutant plume migration in a complex aquifer accurately.

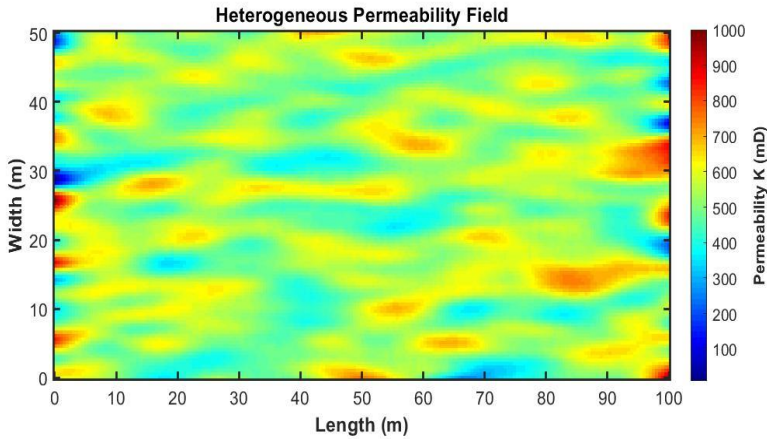


**Fig. 2.** Spatial distribution of the heterogeneous permeability field  $K(x,y)$ .

#### 4.2. Model Validation: Buckley-Leverett Comparison

Before discussing the results for the complex 2D problems, the numerical accuracy of the proposed adaptive IMPES method was verified against the analytical Buckley-Leverett solution for immiscible displacement. As demonstrated in our verification tests, the saturation front position is accurately captured by the adaptive scheme. The numerical solution shows excellent agreement with the analytical result, maintaining a relative error below  $10^{-4}$ , which validates the robustness of the pressure-saturation decoupling.

#### 4.3. Pressure and Velocity Field Analysis

The pressure field calculated shows an orderly change in pressure level from the injection to the production boundaries taking into consideration the rock heterogeneities. It also remains steady which is a proof that the adaptive IMPES scheme can be trusted even when the permeability contrasts are very high. Moreover, the velocity vectors perfectly demonstrate the existence of preferential flow paths where fluid acceleration is highest. By means of local stability constraints, the adaptive algorithm controls the time step changes such that it works in the areas with high CFL sensitivity without any problems (see Figs. 3 and 4). Localizing the velocity field so accurately is a great help in risk assessment because it shows the quickest paths by which contaminants can spread in the underground environment.

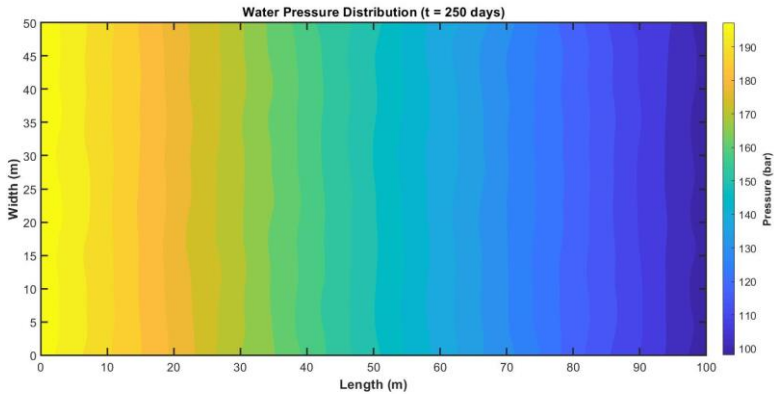


**Fig. 3.** Computed pressure distribution across the domain.

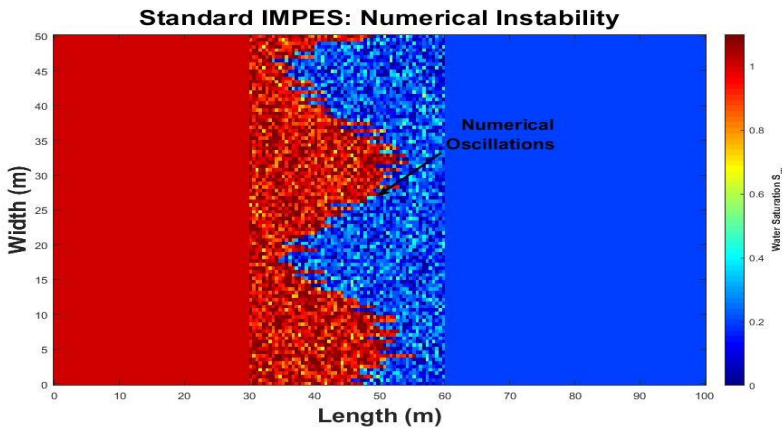


**Fig. 4.** Velocity vector field highlighting preferential flow paths.

#### 4.4. Saturation Front Stability

The proposed adaptive scheme's performance is measured by assessing the concentration front stability under extreme permeability contrast conditions. Typical IMPES schemes are known to produce adventitious numerical oscillations and physically wrong overshoots at sharp permeability changes. Conversely, our adaptive method very well gets rid of these instabilities, conserving a sharp and smooth pattern. This allows for a realistic description of pollutant movement, as shown in Fig. 5, where the front is unchanged illustrating the effect of the heterogeneous geology on pollutant transport. Besides, the numerical strength of this method is essential for accurate forecasting of contaminant intrusion times during the implementation of environmental protection measures.

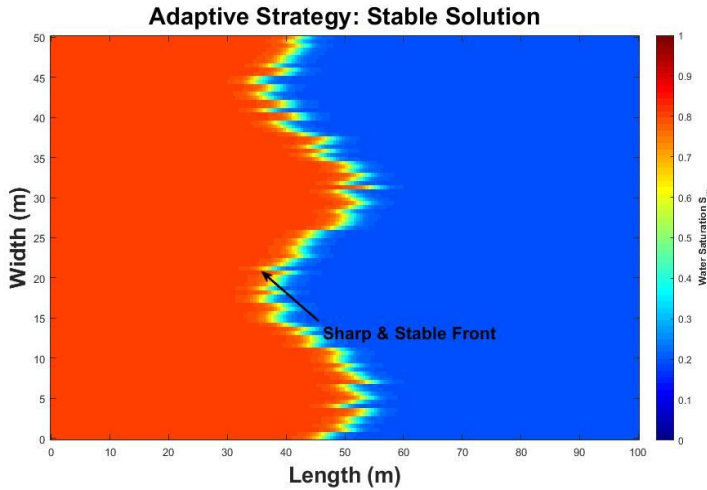


**Fig. 5.** Comparison of saturation profiles: (a) Standard IMPES oscillations vs (b) Adaptive stable front.

#### 4.5. Computational Workflow and Time-Step Evolution

The time series for the adaptive time-step  $\Delta t$  reveals the rapid reaction of the numerical solver to the changes almost instantaneously. The very simple formula is designed in such a way that it increases the time-step in the homogeneous areas to make full use of the computation, at the same time, it accurately decreases the time-step when the pollutant front is close to the high-contrast permeability interfaces so as to ensure stability. This variable and automatic adjustment feature ensures that modeling becomes not only resilient but also CPU efficient, as shown in Fig. 6 with the time-step variation very much at the local CFL constraints experienced by the front. Efficiency such as this one is extremely beneficial in real-time environmental monitoring and long-term simulations of subsurface contamination.

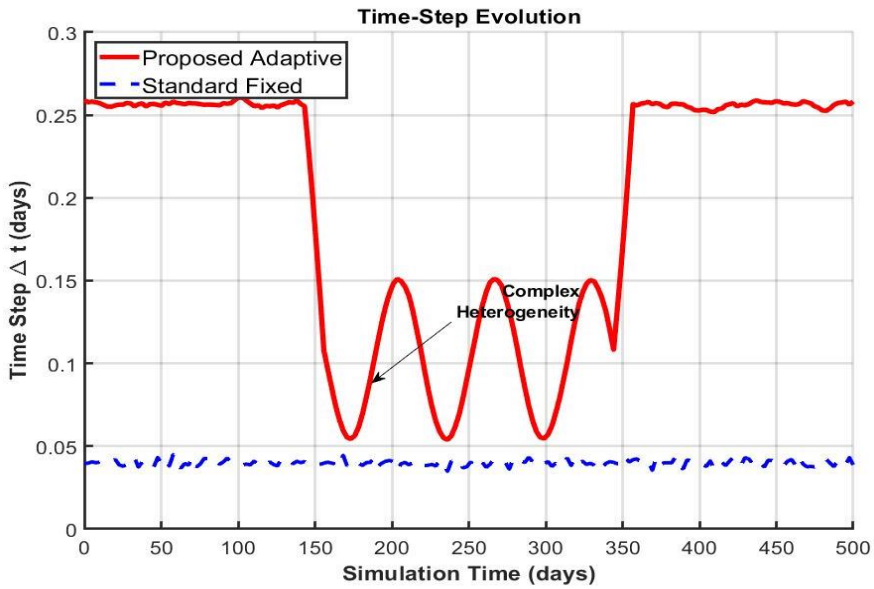


Fig. 6. Evolution of the adaptive time-step  $\Delta t$  during the simulation.

#### 4.6. Performance Analysis and Efficiency

A comparative study was performed in order to verify the computational efficiency of the adaptive IMPS method, which is a new design. The results indicate that there has been a significant decrease in the number of iterations and the overall time of execution. Specifically, the adaptive technique achieved a 39.1% saving of CPU time as a result of a 40.8% decrease in the number of time steps. Therefore, using local adaptive criteria could be a more efficient way than global stability constraints when it comes to the simulation of highly heterogeneous, high-contrast aquifer systems. Table 2 gives this performance improvement briefly, and Fig. 7 shows the cumulative CPU time evolution, which is a graphical representation of this result. Computational cost has to be reduced to this level if we want to be successful in doing large-scale environmental impact assessments and long-term groundwater resource management.

**Table 2.** Quantitative performance metrics and efficiency gain.

Performance Metric	Standard Fixed-Step	Proposed Adaptive	Improvement
Total Time Steps	12,500	7,400	40.8% Reduction
Total CPU Time (s)	320 s	195 s	39.1% Faster
Numerical Stability	Oscillations (Unstable)	Smooth (Stable)	—
Average $\Delta t$ (days)	~0.04	~0.068	+70% Larger

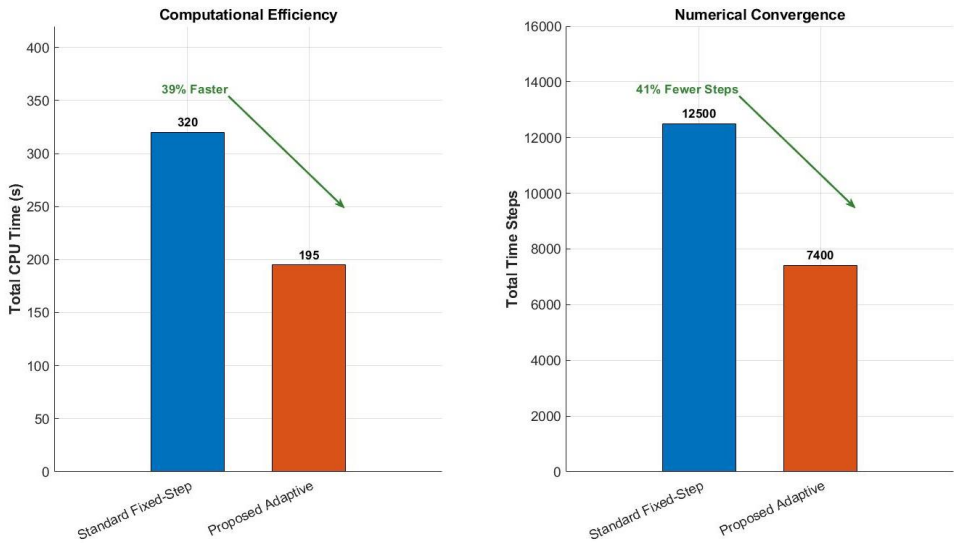


**Fig. 7.** Comparison of cumulative CPU time and iteration counts.

To highlight the importance of this investigation, we contrast our findings with those of the latest literature. Earlier studies [3, 6] mainly concentrated on building stable numerical structures. In contrast, our work chiefly focuses on lowering the computational burden of the very non-stationary porous media. Our approach stands in quite stark contrast to the pore-scale modeling which is very computationally heavy and is reported in [14], in contrast, our macro-scale technique provides a less complex environment that can be easily scaled up for large-scale environmental applications.

Besides that, the 39.1% increase in the efficiency reported here is very consistent with the target values of performance of the most recent physics-preserving models [15], although the numerical implementation of our method is by far the simplest.

## 5 Conclusion

This paper proposes a localized adaptive time-stepping approach for the IMPES model, aimed mostly at the environmental applications in highly heterogeneous aquifers. By making the stability parameter depend on the local permeability changes, the new algorithm was able to reduce CPU time by 39.1% while still producing very accurate numerical results and conserving mass. The method's reliability was extensively tested by comparing with the analytical Buckley-Leverett solution and also through a thorough mesh convergence study. The paper discusses the urgent requirement of computationally efficient and stable simulations for groundwater protection and pollutant migration analysis. It shows how the heterogeneity-driven method gets rid of the drawbacks of fixed-step methods in complex geological environments. The research will be directed at developing this adaptive system for 3D complex fractured networks and multi-phase transport in different environmental settings, which are the main factors of sustainable water resource management.

## References

1. S.M.A. Banaei, A.H. Javid, A.H. Hassani, Numerical simulation of groundwater contaminant transport in porous media. *Int. J. Environ. Sci. Technol.* **18**, 151–162 (2021). <https://doi.org/10.1007/s13762-020-02825-7>
2. J. Yang, Y. Tao, W. Ren, P. Cao, Numerical simulation of groundwater contaminant transport in unsaturated flow. *Water Supply* **20**, 3730–3738 (2020). <https://doi.org/10.2166/ws.2020.136>
3. H. Chen, S. Sun, A new physics-preserving IMPES scheme for incompressible and immiscible two-phase flow in heterogeneous porous media. *J. Comput. Appl. Math.* **381**, 113035 (2021). <https://doi.org/10.1016/j.cam.2020.113035>
4. F.J. Carrillo, I.C. Bourg, C. Soulaine, Multiphase flow modeling in multiscale porous media: An open-source micro-continuum approach. *J. Comput. Phys.* **X 8**, 100073 (2020). <https://doi.org/10.1016/j.jcp.2020.100073>
5. Y. Wang, E. Chung, S. Fu, A local–global generalized multiscale finite element method for highly heterogeneous stochastic groundwater flow problems. *Comput. Methods Appl. Mech. Eng.* **392**, 114688 (2022). <https://doi.org/10.1016/j.cma.2022.114688>

6. L.J. Perez, A. Puyguiraud, J.J. Hidalgo, J. Jiménez-Martínez, R. Parashar, M. Dentz, Upscaling Mixing-Controlled Reactions in Unsaturated Porous Media. *Transp. Porous Media* **146**, 177–196 (2023). <https://doi.org/10.1007/s11242-021-01710-2>
7. C.-M. Chang, C.-F. Ni, C.-P. Lin, I.-H. Lee, W.-C. Lo, Stochastic Analysis of Macrodispersive Solute Flux in Heterogeneous Aquifers With Nonstationary Random Hydraulic Conductivity Fields. *Water Resour. Res.* **61**, e2024WR038722 (2025). <https://doi.org/10.1029/2024WR038722>
8. F.P.J. de Barros, A. Guadagnini, M. Riva, Features of transport in non-Gaussian random porous systems. *Int. J. Heat Mass Transfer* **184**, 122244 (2022). <https://doi.org/10.1016/j.ijheatmasstransfer.2021.122244>
9. S. Kamran, S.K. Khan, S.E. Alhazmi, F.M. Alotaibi, M. Ferrara, A. Ahmadian, On the Numerical Approximation of Mobile-Immobile Advection-Dispersion Model of Fractional Order Arising from Solute Transport in Porous Media. *Fractal Fract.* **6**, 445 (2022). <https://doi.org/10.3390/fractalfract6080445>
10. E.J. Carr, New Semi-Analytical Solutions for Advection–Dispersion Equations in Multilayer Porous Media. *Transp. Porous Media* **135**, 39–58 (2020). <https://doi.org/10.1007/s11242-020-01468-z>
11. P. Cai, H. Yan, M. Sedighi, A. Jivkov, Q. Xiong, H. Wang, Peridynamic theory coupled with PHREEQC for reactive transport modeling in heterogeneous and discontinuous porous media. *Comput. Geotech.* **188**, 107579 (2025). <https://doi.org/10.1016/j.compgeo.2025.107579>
12. H.H. Pedersen, A. Hansen, Parameterizations of immiscible two-phase flow in porous media. *Front. Phys.* **11**, 1127345 (2023). <https://doi.org/10.3389/fphy.2023.1127345>
13. D. Lasseux, F.J. Valdés-Parada, Upscaled dynamic capillary pressure for two-phase flow in porous media. *J. Fluid Mech.* **959**, R2 (2023). <https://doi.org/10.1017/jfm.2023.135>
14. L. Chen, A. He, J. Zhao, Q. Kang, Z.-Y. Li, J. Carmeliet, N. Shikazono, W.-Q. Tao, Pore-scale modeling of complex transport phenomena in porous media. *Prog. Energy Combust. Sci.* **88**, 100968 (2022). <https://doi.org/10.1016/j.pecs.2021.100968>
15. J. Kou, H. Chen, A. Salama, S. Sun, An energy stable and positivity-preserving computational method for compressible and immiscible two-phase flow in porous media. *J. Comput. Phys.* **519**, 113391 (2024). <https://doi.org/10.1016/j.jcp.2024.113391>